J. Fluid Mech. (1969), *vol.* 38, *part* 4, *pp.* 817–831
Printed in Great Britain

Sink flow turbulent boundary layers

By B. E. LAUNDER AND W. P. JONES
Department of Mechanical Engineering, Imperial College, London, S.W. 7

(Received 7 January 1969)

The study of sink flow turbulent boundary layers is of particular relevance to the problem of laminarization. The reason lies in the fact that the acceleration parameter which principally determines when a turbulent boundary layer will begin to revert towards laminar is, in these flows, constant from station to station. The paper presents theoretical solutions to this class of boundary layer by making use of the Prandtl mixing-length formula to relate the turbulent shear stress to the mean velocity gradient. Near the wall the Van Driest recommendation for mixing length is adopted and the Van Driest function, A^+, is chosen such that the skin friction coefficient does not exceed a certain maximum value.

The predicted solutions, which are in good agreement with available experimental data, display a plausible shift from the turbulent towards the laminar solution as the acceleration parameter is increased.

1. Introduction

The flow that develops in a convergent channel between intersecting planes is one that has attracted considerable attention over the years. For laminar flow, similar solutions of the complete Navier–Stokes equations have been obtained (Jeffrey 1915; Hamel 1917; Rosenhead 1940; and Millsaps & Pohlhausen 1953) and, in the limit of very high Reynolds numbers, these reduce to the exact boundary-layer solution of Pohlhausen (1921).

In turbulent flow, it is the only flow configuration with a varying free-stream velocity in which the characteristic viscous and turbulence length scales may develop at the same rate; thus, since similar laminar flows are attainable, completely similar turbulent flows may also be achieved. For both laminar and turbulent flow these sink flow similar boundary layers have skin friction coefficients and local Reynolds numbers which are invariant with x.

For these sink flows, the acceleration parameter K (defined as $(\nu/U^2)\,dU/dx$) is also a constant at all stations in the flow. Launder (1964*a*, 1964*b*), Moretti & Kays (1965), Patel (1965), Schraub & Kline (1965) found experimentally that the parameter K provided a useful indication of when an accelerated turbulent boundary layer would undergo reversion towards laminar. To the accuracy that K determines the onset of laminarization, the critical value may be taken as $2{\cdot}5 \times 10^{-6}$.

A number of authors have attempted to derive from simple theoretical arguments the parameter which controls laminarization. The most popular 'local' parameter is $(\nu/\rho u_\tau^3)dp/dx$ (which, except for a multiplicative constant,

is identical with $Kc_f^{-\frac{3}{2}}$). Recently Patel & Head (1968) have suggested that the local pressure gradient, which appears in the above term, should be replaced by the mean shear-stress gradient over a region near the wall $\overline{\partial\tau/\partial y}$; they therefore proposed the group $(\nu/\rho u_\tau^3)\overline{\partial\tau/\partial y}$. While such a parameter is, conceptually, an improvement on earlier recommendations there is some uncertainty in deciding over what inner fraction of the boundary layer the shear-stress gradient should be averaged. Moreover, from an experimental standpoint, it is a formidable task to measure with accuracy shear-stress gradients near the wall in accelerated turbulent boundary layers. Fortunately, in sink flows, the question of precisely which parameter brings about laminarization is not important since K, $Kc_f^{-\frac{3}{2}}$ and the Head–Patel parameter are all constant.

The work of Schraub & Kline (1965) first suggested that the study of sink flow boundary layers might be of special relevance to the problem of laminarization. They examined the sublayer structure of accelerated turbulent boundary layers by means of dye-injection and hydrogen-bubble techniques. They found that the sinuous low momentum sublayer streaks which are a feature of turbulent boundary layers on smooth surfaces did not suddenly cease to form above a certain level of acceleration. Instead they suffered a *progressive* diminution as the value of K was steadily increased.

Although Schraub & Kline's measurements were made in boundary-layer flows in which K varied in the x direction, the region of the boundary layer under study was so close to the surface that the flow would have been nearly in local equilibrium. It thus appeared probable that, by establishing experimentally similar sink flows, one could examine a family of turbulent boundary layers displaying, for progressively larger values of K, features which became more and more akin to those of a laminar boundary layer. It was for this reason that Launder & Stinchcombe (1967) set up three similar boundary layers for values of K of $0{\cdot}7 \times 10^{-6}$, $1{\cdot}3 \times 10^{-6}$, and $3{\cdot}0 \times 10^{-6}$. The mean velocity profiles which are shown in figure 1 clearly display the shift towards the laminar solution with increasing K. Even at the largest value of K, however, it is seen from figure 2, there existed a large, self-preserving u' component of turbulence. The boundary layer was still essentially turbulent.

The measurements of Launder & Stinchcombe have a number of shortcomings. Undertaken for a short-term research project, they lack both the breadth and the precision that one would like. In particular the flow along the test plate was diverging slightly and consequently, for a given value of K, the boundary layers display a greater departure from the structure of a normal turbulent boundary layer than they would have, had the flow been strictly two-dimensional. Their measurements confirmed, however, the implication of Schraub & Kline's work, namely that, over a limited range of accelerations, turbulent boundary layers may occur which display marked differences in structure (particularly within the sublayer), from those, say, of a flat-plate boundary layer. Nevertheless, the boundary layers are *essentially* turbulent since they are not in transit from the turbulent to the laminar state. Following Schraub & Kline, these boundary layers are here described as 'laminarescent'.

The present contribution is principally concerned with the numerical solution

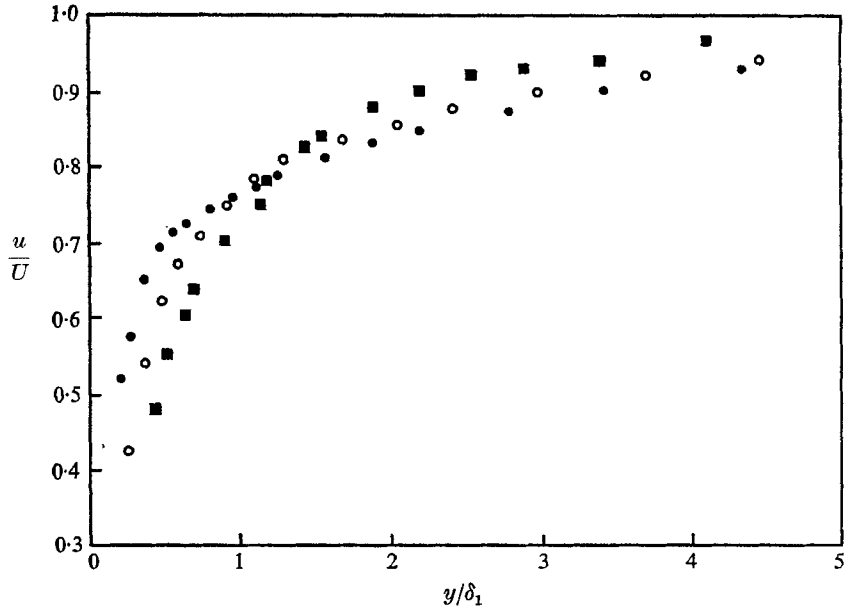

FIGURE 1. Mean velocity profiles in sink flow boundary layers, Launder & Stinchcombe (1967). ■, $R_2 = 200$, $K = 3 \times 10^{-6}$; ○, $R_2 = 390$, $K = 1{\cdot}3 \times 10^{-6}$; ●, $R_2 = 990$, $K = 0{\cdot}7 \times 10^{-6}$.

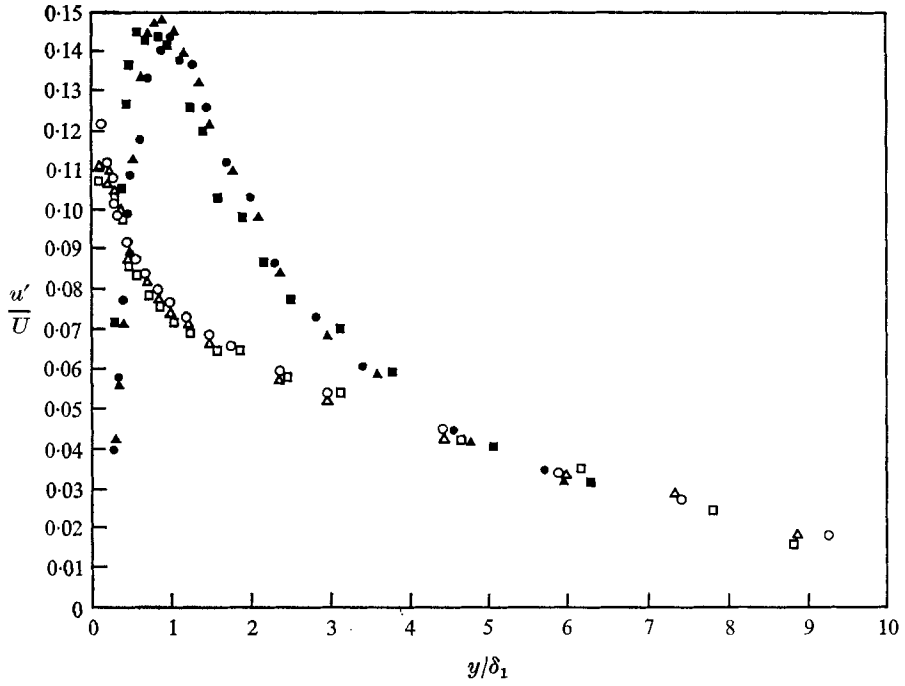

FIGURE 2. Longitudinal turbulence intensity profiles, Launder & Stinchcombe (1967). Distance from wedge entry: ○, 21 in.; △, 23 in.; □, 25 in.; ○, $K = 0{\cdot}7 \times 10^{-6}$; ●, $K = 3 \times 10^{-6}$.

of the Reynolds equations for sink flow turbulent boundary layers. The solutions are obtained by using the mixing-length hypothesis to relate the turbulent shear stress to the mean velocity gradient. In particular, the Van Driest (1956) specification of mixing length is adopted throughout the wall region. The chosen momentum-transport model yields predictions in satisfactory agreement with measurement for values of K up to about 10^{-6}.

For steeper accelerations, it is shown that, by allowing the Van Driest 'constant', A^+, to increase with K, the model yields plausible predictions of the mean velocity profile, R_2 and H, for laminarescent boundary layers.

2. Outline of the analysis

A complete analysis is contained in the appendix; here, merely the principal steps will be given.

Townsend (1956) has demonstrated that, for a plane sink flow, the boundary-layer momentum and continuity equations for a constant-properties turbulent fluid may be reduced to an ordinary differential equation in terms of a similarity variable proportional to Uy/ν. This equation may be written

$$1-f^2+f''+K^{-\frac{1}{2}}S' = 0, \tag{1}$$

where f is the normalized velocity u/U, S is the normalized Reynolds shear stress $-\overline{u'v'}/U^2$ and primes denote differentiation with respect to the similarity variable η, defined as $(Uy/\nu)\,K^{\frac{1}{2}}$.

The Prandtl mixing-length hypothesis is used to relate the turbulent shear stress, $-\rho\,\overline{u'v'}$, to the mean velocity gradient. Although there are well-founded physical grounds for discarding this momentum-transport model there are two reasons why its use in the prediction of sink flow boundary layers may be acceptable. First, the boundary layers are similar from station to station and the objection that Prandtl's mixing-length hypothesis does not permit the shear-stress profile to 'float' freely from the velocity profile is not important. Moreover, in the outer region of the boundary layer where confidence in the mixing-length theory breaks down, the shear stresses are so much smaller than the wall shear stress that an imperfect specification of mixing length has only a small effect on the predicted boundary-layer profile.

Over a region near the wall, the Van Driest (1956) specification of mixing length, l, is adopted,

$$l = ky\,(1-\exp\,(-y^+/A^+)). \tag{2}$$

It is evident from (2) that A^+ may be interpreted as a dimensionless sublayer thickness. Van Driest proposed that A^+ should be a constant (equal to 26) and a set of solutions have been obtained for this value of A^+. However, a number of workers have found from experiments on strongly accelerated turbulent boundary layers that the most obvious change in structure of a boundary layer reverting towards laminar was that the viscous sublayer grew appreciably (in terms of y^+). Accordingly, further solutions (and these form the main con-

tribution of the present paper) were computed for which A^+ increased with K. The basis of the $A^+(K)$ variation is given in the following section.

Over the outer part of the layer the mixing length was assumed to be constant, equal to about 10% of the boundary-layer thickness. Moreover, the viscous term, f''', in (1) was neglected. The omission of this term greatly simplified the task of obtaining numerical solutions to the boundary-layer equation for an analytic solution to the outer region was then possible. Standard iterative procedures could then be adopted for matching the numerical solution for the inner region to the analytic form for the outer region.

3. Presentation and discussion of results

Solutions with A^+ constant

Figures 3 and 4 display comparisons of predicted sink flow velocity profiles with experimental data. The predicted profiles are those obtained by setting A^+ equal to 26. Figure 3 shows the mean velocity profiles on linear f, η axes; the laminar solution of Pohlhausen (1921) is also shown. The experimental data are those of Herring & Norbury (1967) and Jones (1967).

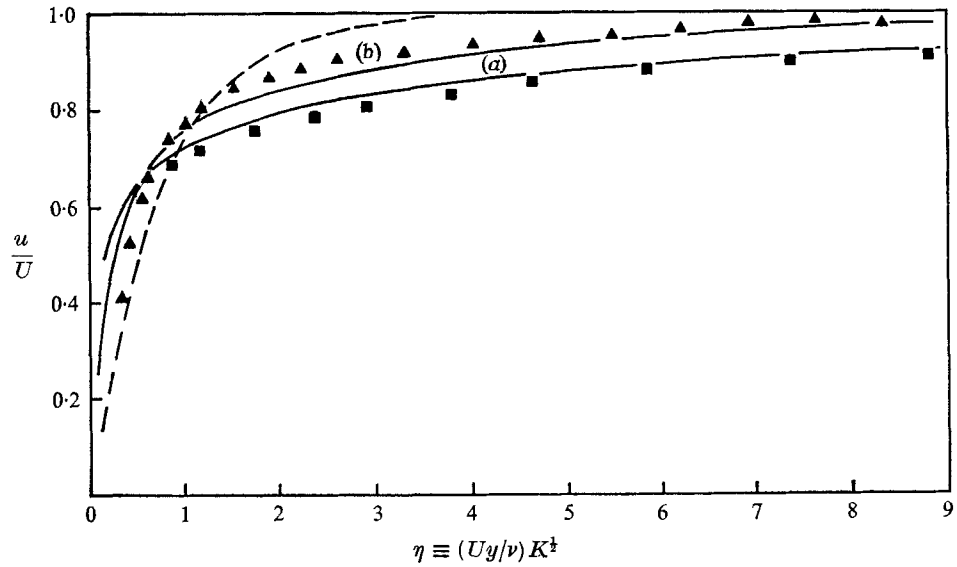

FIGURE 3. Mean velocity profiles for sink flow boundary layers. ■, Herring & Norbury; ▲, Jones. — —, laminar solution: (*a*) ——, $K = 2{\cdot}4 \times 10^{-7}$; (*b*) ——, $K = 2{\cdot}2 \times 10^{-6}$.

The Herring & Norbury data were of 'equilibrium' rather than 'similar' boundary layers so some explanation is needed to justify using their results in the comparison. Formally, an equilibrium boundary layer is one which has developed for sufficient time in a pressure gradient whose magnitude is adjusted so that the parameter β (defined as $-(\delta_1/\tau_w)\,dp/dx$) is constant at all stations in the flow. When the equilibrium state is reached, all of the velocity profile outside

the viscous layer is self-preserving when plotted in velocity-defect co-ordinates. It is noted that

$$\beta \equiv 2KR_2H/c_f. \tag{3}$$

Thus similar sink flow boundary layers are a particular subset of equilibrium boundary layers; flows in which each of the parameters on the right side of equation (3) are separately constant. Mellor & Gibson (1963) originally suggested that equilibrium boundary layers could not be obtained for values of β greater than 0·5. Launder & Stinchcombe (1967) showed, however, that $\beta = 0{\cdot}5$ was merely a dividing line between two types of equilibrium boundary layer.

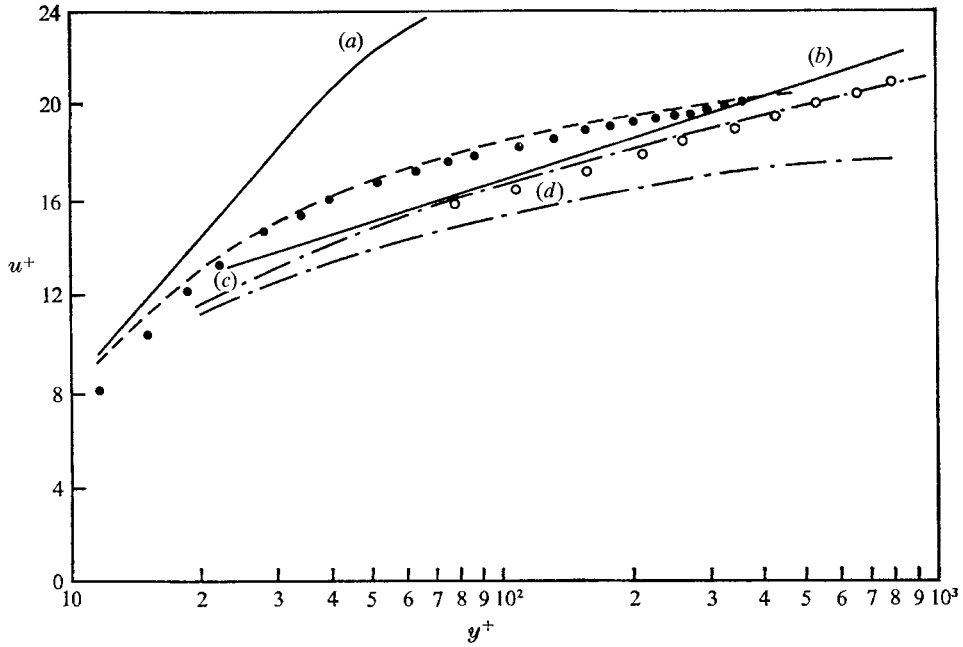

FIGURE 4. Mean velocity profiles, universal co-ordinates. ●, Jones; ○, Herring & Norbury. Curves: (*a*) ——, laminar: (*b*) ——, $u^+ = 1/k \ln y^+ + c$: - - -, $K = 2{\cdot}2 \times 10^{-6}$, $A^+ = 61$; (*c*) —·—, $K = 2{\cdot}4 \times 10^{-7}$, $A^+ = 26$; (*d*) —·—, $K = 2{\cdot}2 \times 10^{-6}$, $A^+ = 26$.

For $\beta < 0{\cdot}5$, the Reynolds number would increase indefinitely with x; for $\beta > 0{\cdot}5$, the boundary layer would approach asymptotically the similar sink flow condition. The Herring & Norbury data shown in figure 3, for which $\beta = 0{\cdot}53$, fall into the latter category. Moreover, an examination of their tabulated data implied that dR_2/dR_x was insignificant compared with the other terms in the momentum-integral equation† at their last measuring station. Thus the velocity profile at this station (which is the one plotted in figure 3) may reasonably be assumed to be very close to similar.

It is seen from figure 3 that the data of Herring & Norbury are, indeed, well predicted by the theoretical solution. Agreement is less satisfactory, however, with Jones's data at $K = 2{\cdot}2 \times 10^{-6}$. The discrepancy between measurement and

† The momentum-integral equation may be written: $dR_2/dR_x + R_2K(H+1) = \frac{1}{2}c_f$.

prediction is greatest near the wall, where the slope of the theoretical profile is considerably greater than the measured.

The above discrepancy is shown in sharper relief in figure 4, where theoretical and experimental profiles are plotted semi-logarithmically on u^+, y^+ axes. The laminar solution and the universal profile

$$u^+ = (1/0{\cdot}4)\ln y^+ + 5{\cdot}3 \qquad (4)\dagger$$

are also plotted. At $K = 0{\cdot}24 \times 10^{-6}$, the predicted profile and the data of Herring & Norbury lie close to equation (4). At $K = 2{\cdot}2 \times 10^{-6}$ the predicted profile lies somewhat below equation (4) but the measured solution lies considerably above it; that is, the effective sublayer thickness of the measured solution is significantly thicker than that of the predicted profile.

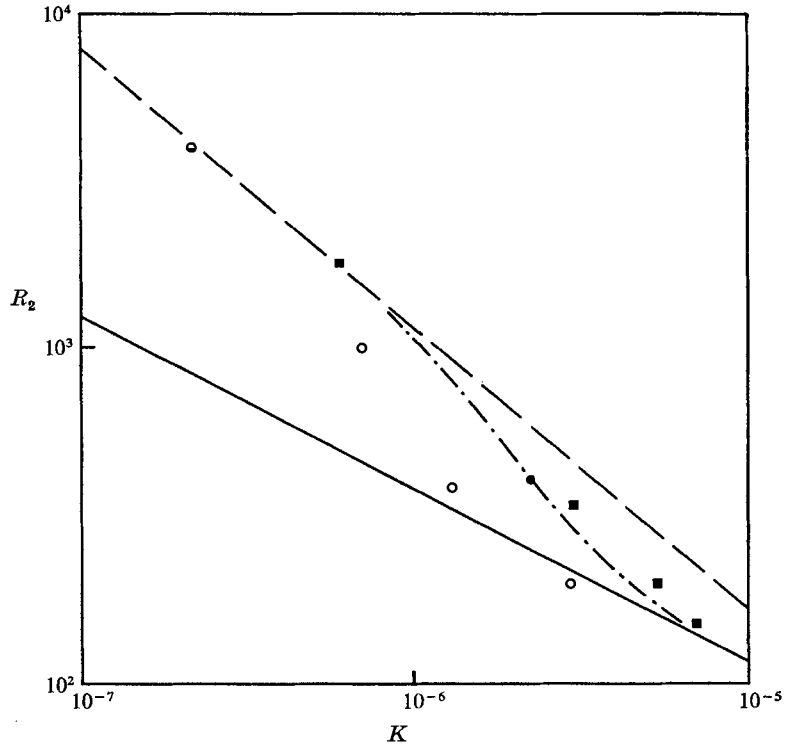

FIGURE 5. Variation of momentum deficit thickness Reynolds number with K. ◒. Herring & Norbury; ■, Badri Narayanan; ○, Launder & Stinchcombe; ●, Jones ——, laminar solution; — —, turbulent solution, $A^+ = 26$; — · —, turbulent solution, $A^+ = f(L)$.

Further evidence of the respective successes and shortcomings of the predicted solutions is presented in figures 5 and 6. Since R_2 and H are constant for a given value of K, a single point on these graphs corresponds to a particular sink flow boundary layer. Here, attention is focused on the predicted solution for $A^+ = 26$

† 5·3 is the additive constant in the universal law implied by the choice of $k = 0{\cdot}40$ and $A^+ = 26$.

marked by a dashed line. In figure 5, the Herring & Norbury data and those of Badri Narayanan & Ramjee (1968) for their mildest acceleration lie very close to the predicted turbulent solution. Jones's data, however, lie midway between the turbulent and laminar solutions as do those of Badri Narayanan & Ramjee for their steeper accelerations (though, with the latter data, it seems doubtful whether the boundary layers had truly reached their self-preserving condition). The earlier data of Launder & Stinchcombe (1967) are also shown and clearly display the shift of the measured boundary layer from turbulent towards laminar as K is increased. In fact, the indicated shift is too great because, as mentioned in §1, these boundary layers were not two-dimensional. Thus, at $K = 3 \times 10^{-6}$, their measured momentum-thickness Reynolds number was marginally *less* than the laminar solution although, as was seen in figure 2, a self-preserving turbulence intensity distribution existed in these layers.

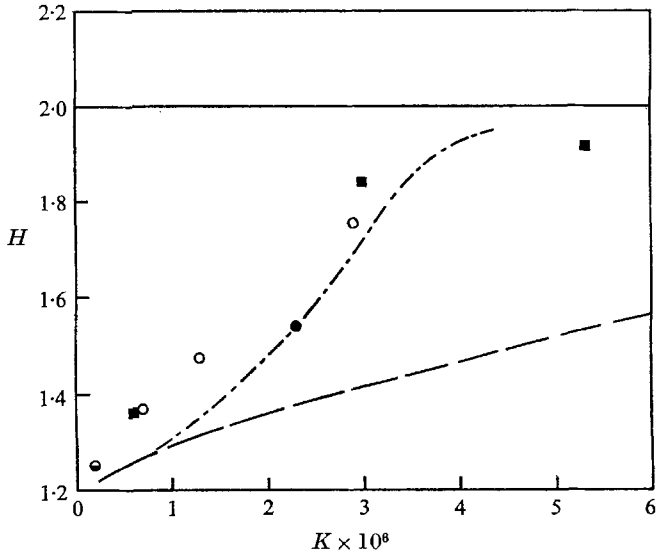

FIGURE 6. Variation of shape factor with K. ■, Badri Narayanan; ○, Launder & Stinchcombe; ●, Jones; ◒, Herring & Norbury. ——, laminar solution; — · —, $A^+ = f(L)$; — —, $A^+ = 26$.

The predicted and measured variation of the shape parameter, H, with K is shown in figure 6. Because the viscous sublayer has been included in the theoretical solution the shape factor increases with K. The rise in H, however, is not nearly as rapid as that of the measured solutions. In this figure the data of Launder & Stinchcombe do not appear as anomalous as they do in figure 5. This result is in accordance with expectations for it would be anticipated that the divergence of the flow would have a greater effect on the Reynolds number than on the shape of the boundary layer.

Solutions with A^+ dependent upon L

The above comparisons with data have shown the predicted solutions to be in close agreement with measurements for values of K up to about 10^{-6}. For

higher values of K, the data show a progressive shift towards the laminar boundary-layer solution. Indeed, the data on figure 6 would seem to suggest that no non-laminar solution exists for a value of K in excess of 4×10^{-6} (and this value is in agreement with the measurements of Schraub & Kline (1965), who found that the sublayer streaks ceased to form when K was greater than $3{\cdot}5 \times 10^{-6}$).

Figure 4 had shown clearly that one important shortcoming of the theoretical solution was that no means were incorporated to allow the region over which viscous effects were important to grow as K increased.† Since the boundary layers were essentially turbulent, however, it seemed worth investigating

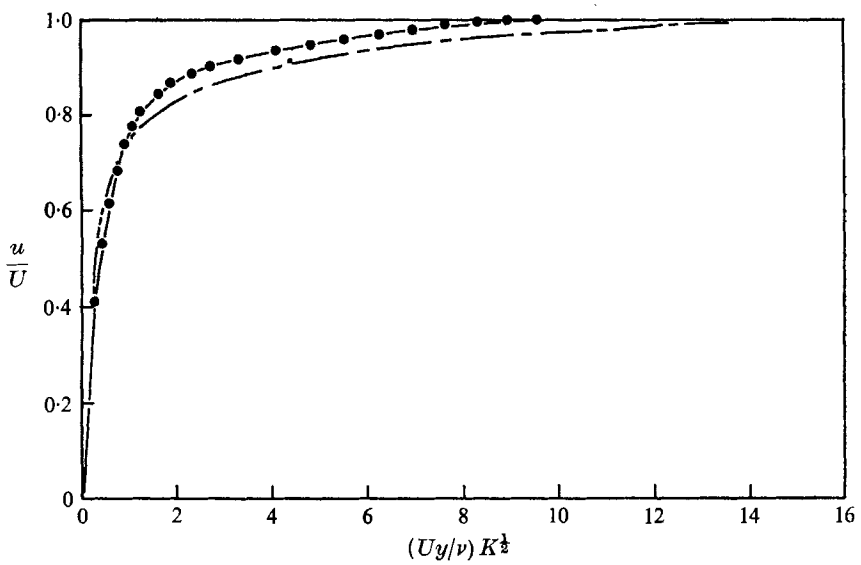

FIGURE 7. Mean velocity profiles, experimental and predicted solution to sink flow boundary layer; $K = 2{\cdot}2 \times 10^{-6}$. ●, Jones, $K = 2{\cdot}2 \times 10^{-6}$. ——, $A^+ = 61$; – · –, $A^+ = 26$.

whether by increasing A^+ one could obtain solutions in tolerable agreement with experiment. A solution of equation (8) was thus recomputed with $K = 2{\cdot}2 \times 10^{-6}$ and A^+ chosen (by trial and error) such that the predicted profile had the same momentum-thickness Reynolds number as Jones's measured solution, i.e. $R_2 = 430$. The required value of A^+ was 61 and in figures 4 and 7 the theoretical and measured velocity profiles are plotted. The result surpassed expectations for the complete experimental profile was indistinguishable from that predicted with $A^+ = 61$. In principle, it would be feasible to establish very many sink flow boundary layers and determine empirically the value of A^+ which generated the same theoretical Reynolds numbers as the measured profiles. In the absence of further experimental information, however, it is necessary to speculate how A^+ may depend on K or, equivalently, on $L(Kc_f^{-\frac{3}{2}})$.

† There is also a considerable amount of data reported for *non*-similar turbulent boundary layers showing a similar thickening of the sublayer (Launder 1964, Patel 1965, Schraub & Kline 1965, Patel & Head 1968, and Badri Narayanan & Ramjee 1968).

Coles (1962) has remarked that the maximum value of skin friction coefficient that a turbulent boundary layer in zero pressure gradient can attain appears to be about 0·0048. Although the connexion with these boundary layers appeared rather tenuous, it seemed notable that this was the implied value of c_f for Jones's sink flow measurements. Moreover, like sink flow boundary layers, low Reynolds number turbulent flows in zero pressure gradient have no wake-component in their velocity profile. Thus the similarity of these two types of boundary layer may be closer than it would superficially appear to be. It was therefore assumed that, in sink flow layers, the viscous sublayer grew in thickness to prevent the skin friction coefficient exceeding this critical value. With this constraint imposed, solutions were recomputed to determine the variation of A^+ with L. The calculated values of A^+ are plotted in figure 8; it is seen they are well correlated by the equation

$$\left.\begin{aligned} L &\leqslant 1{\cdot}9\times10^{-3},\ A^+ = 26;\\ L &> 1{\cdot}9\times10^{-3},\ A^+ = 11+7{\cdot}9\times10^{3}L. \end{aligned}\right\} \tag{5}$$

The predicted variations of R_2 and H with K, with A^+ calculated from (5), are represented by the chain lines in figures 5 and 6. The predictions display a plausible shift from the turbulent to the laminar solution as K increases.

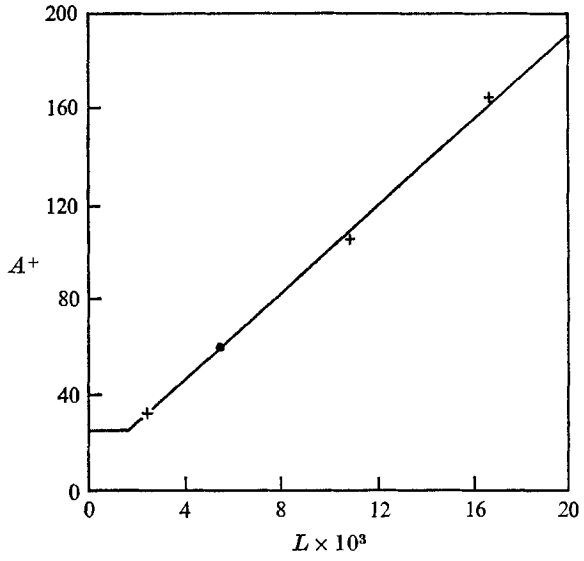

FIGURE 8. Provisional $A^+(L)$ function for sink flow boundary layers. ●, Jones.

Conclusions

Theoretical solutions have been obtained to sink flow turbulent boundary layers by using the mixing-length hypothesis to relate the shear stress to the mean velocity gradient. For modest accelerations ($K < 10^{-6}$) good agreement with experimental data is obtained by taking the Van Driest sublayer function, A^+, equal to 26. For steeper accelerations, it has been shown that, by allowing A^+ to increase with K such that the skin friction coefficient remains constant,

the theoretical solutions display a progressive shift towards the laminar solution in good agreement with existing data of sink flow laminarescent boundary layers.

Appendix. Analysis

The two-dimensional momentum and continuity equations for an incompressible turbulent boundary layer are:

$$\frac{u\partial u}{\partial x}+\frac{v\partial u}{\partial y}=\frac{UdU}{dx}+\frac{\nu\partial^2 u}{\partial y^2}-\frac{\partial\overline{u'v'}}{\partial y}-\frac{\partial}{\partial x}(\overline{u'^2}-\overline{v'^2}), \tag{A 1}$$

$$\frac{\partial u}{\partial x}+\frac{\partial v}{\partial y}=0. \tag{A 2}$$

Townsend (1956) has demonstrated that, for flow between converging planes, equations (A 1) and (A 2) are reducible to an ordinary differential equation in terms of a similarity variable proportional to Uy/ν. With the following normalizations:

$$f(\eta)\equiv u/U,\quad S(\eta)\equiv -\overline{u'v'}/U^2,\quad N(\eta)\equiv -(\overline{u'^2}-\overline{v'^2})/U^2,\quad \eta\equiv K^{\frac{1}{2}}(yU/\nu),$$

equations (A 1) and (A 2) may be expressed

$$1-f^2+f''+K^{-\frac{1}{2}}S'+2N+N'=0 \tag{A 3}$$

with boundary conditions $f(0)=0$ and $f(\infty)=1$.

With the above choice of variables, it is easily demonstrated that

$$R_2=K^{-\frac{1}{2}}\int_0^\infty f(1-f)\,d\eta \quad\text{and}\quad c_f=2K^{\frac{1}{2}}f'(0);$$

thus, as Townsend (1956) has remarked, the skin friction coefficient and any local length-scale Reynolds number are invariant with x.

Solutions to equations (A 3) will yield a family of velocity profiles for various values of the parameter K. Indeed, with the above choice of similarity variable, the laminar solution (i.e. S and N equal to zero), is independent of K; hence laminar *and* turbulent boundary layers together comprise a unique one-parameter set of sink flow solutions.

In obtaining solutions to (A 3) below, the Reynolds normal stress, N, and its derivative have been neglected. This is a usual assumption in turbulent boundary-layer analysis and is analogous to the neglect of streamwise molecular diffusion for laminar flow. The terms have been included this far merely to demonstrate that their retention did not affect the existence of similar solutions. Prandtl's mixing-length hypothesis is used to relate the turbulent shear stress to the mean velocity gradient.

Thus it is assumed that

$$-\overline{u'v'}=l^2\left|\frac{\partial u}{\partial y}\right|\left(\frac{\partial u}{\partial y}\right), \tag{A 4}$$

where the variation of the mixing length, l, across the boundary layer must be assigned.

Throughout a region close to the surface, Van Driest's (1956) recommendation for the variation of mixing length is adopted:

$$l = ky[1-\exp(-y^+/A^+)] \quad (0 \leqslant y \leqslant y_j), \tag{A 5}$$

where the value of y_j is chosen below. Van Driest found that, with k and A^+ assigned the values 0·40 and 26 respectively, (A 4) and (A 5) predicted mean velocity profiles in turbulent pipe flow which were in excellent agreement with measured values throughout the sublayer and logarithmic regions of the flow. Here the above value of k is retained but in § 3 the effect of letting A^+ depend upon the acceleration parameter K is examined. The region of the boundary layer over which (A 5) is applied is henceforth called the 'inner region'; correspondingly, the flow at distances from the wall greater than y_j is termed the 'outer region'.

For the outer region, the viscous term in (A 3), f''', is neglected. With this simplification, the use of the mixing-length hypothesis leads to a definite outer edge to the boundary layer. It is known from experiment that rotational turbulent fluid ceases at a finite height above the surface and so a finite edge to the theoretical solutions conforms with reality. Moreover, the neglect of f''' leads, as is seen, to a great simplification in the task of obtaining solutions to (A 3). The outer boundary condition of (A 3) thus becomes $f(\eta_\delta) = 1$ where η_δ is the value of the similarity variable at the edge of the layer. Since η_δ is unknown, however, the further constraint that $f'(\eta_\delta) = 0$ is applied to enable its value to be determined.

Escudier (1964) found, from an examination of a diversity of turbulent boundary layers (but not including severely accelerated flows), that the mixing length over the outer 80 % of the boundary layer was reasonably constant and equal to about 10 % of the layer's thickness. Here the value of y_j is set equal to $(\lambda\delta/k)$ and the assumed constant value of mixing length over the outer region is

$$l = M\lambda\delta \quad (y_j < y \leqslant \delta). \tag{A 6}$$

In the solutions presented below, λ is assigned the value of 0·09 and the value of M is chosen to give a continuous shear stress at the join; its value is determined from the expression

$$\left\{\frac{\mu}{\rho} + [ky(1-\exp(-y^+/A^+)]^2\left|\frac{\partial u}{\partial y}\right|\right\}_j = \left\{(M\lambda\delta)^2\left|\frac{\partial u}{\partial y}\right|\right\}_j. \tag{A 7}$$

In practice, M differs negligibly from unity for values of K up to 10^{-6}. Moreover, for sink flow boundary layers, $\partial u/\partial y$ is always positive so the magnitude signs in (A 4) and (A 7) may be dropped.

When the turbulent shear-stress formulation implied by (A 4), (A 5) and (A 6) is cast into dimensionless form there results:

$$\text{inner region } (0 \leqslant \eta \leqslant \eta_j): \quad S = [k\eta(1-\exp t)f']^2; \tag{A 8}$$

$$\text{outer region } (\eta_j < \eta \leqslant \eta_\delta): \quad S = (M\lambda\eta_\delta f')^2; \tag{A 9}$$

where $t \equiv -\eta(c_f/2K)^{\frac{1}{2}}/A^+$.

Expressions for S' are obtained by differentiating (A 8) and (A 9) with respect to η and these are then substituted in the momentum equation. The following two second-order equations in f result:

$$0 \leqslant \eta \leqslant \eta_j: \quad \{f'' + 2k^2K^{-\frac{1}{2}}[T_2(f'^2 + f'f''\eta) + T_3T_4f'^2]\} \times (1 - k^2\eta^3f''^2T_3/T_4)^{-1} + 1 - f^2 = 0, \quad \text{(A 10)}$$

where

$$T_1 = \exp(t),$$
$$T_2 \equiv (1 - T_1)^2,$$
$$T_3 \equiv (1 - T_1)\,T_1/(A + K^{\frac{1}{2}}),$$
$$T_4 \equiv (S + K^{\frac{1}{2}}f')^{\frac{1}{2}},$$

where S is given by (A 8),

$$\eta_j < \eta \leqslant \eta_\delta: \quad 1 - f^2 + 2K^{-\frac{1}{2}}(M\lambda\eta_\delta)^2 f'f'' = 0. \quad \text{(A 11)}$$

The numerical solution of (A 10) and (A 11) would normally be an arduous business. To start the solution, one would need to guess $f'(0)$ and η_δ. The numerical solution would then have to be performed many times, iterating on both these variables, until the outer boundary conditions $f(\eta_\delta) = 1$ and $f'(\eta_\delta) = 0$ were satisfied. However, an analytic solution to (A 11) was found:

$$(1 - \eta/\eta_\delta) = [2\lambda^2M^2/K^{\frac{1}{2}}\eta_\delta]^{\frac{1}{2}}\left\{\sqrt{3}(\pi/2 - \tan^{-1}[(2z-1)/\sqrt{3}]) - \tfrac{1}{2}\ln\left[\frac{1 - z + z^2}{(1+z)^2}\right]\right\}, \quad \text{(A 12)}$$

where $z \equiv [(2+f)/(1-f)]^{\frac{1}{3}}$ and the term within the curly brackets on the right of (A 12) is merely

$$3\int_z^\infty z/(1+z^3).$$

This discovery much simplified the task of obtaining numerical solutions to the inner region of the boundary layer; the procedure was as follows. Equation (A 11) was multiplied by f' and integrated between η_j and η_δ. After some rearrangement the result was expressed:

$$\left.\begin{aligned} G(\eta)|_j &= 2K^{-\frac{1}{2}}, \\ \text{where} \qquad G(\eta) &\equiv [(1-f)^2(2+f)]/[f'^3(M\lambda\eta_\delta)^2]. \end{aligned}\right\} \quad \text{(A 13)}$$

With a guessed value of $f'(0)$, (A 10) was integrated outwards across the layer by a fourth-order Runge–Kutta procedure. Once the solution had proceeded beyond the viscous sublayer, $G(\eta)$ was computed at each step to determine whether its value was greater or less than $2K^{-\frac{1}{2}}$. If it was greater, the solution proceeded another step; if it was less, the computation was halted and the current value of η was ascribed to η_j. In fact, as $G(\eta)$ became close to $2K^{-\frac{1}{2}}$, the step size was progressively reduced so that η_j was determined accurately. One thus obtained an implied value for the boundary-layer thickness, η_δ, i.e. $\eta_{\delta a} = k\eta_j/\lambda$.

From (A 12), however, a second implied value for the layer thickness, $\eta_{\delta b}$, could be obtained by replacing η/η_δ by λ/k and substituting the value of f obtained above for the inner solution at η_j. Unless the guessed value of $f'(0)$ had been correct $\eta_{\delta a}$ and $\eta_{\delta b}$ would differ. However, by standard iteration procedures the correct solution could rapidly be extracted.

It is worth noting that a very simple analytic solution to the outer region is obtained if equation (A 11) is partially linearized. With the substitution $(1-e) \equiv f$ and f^2 approximated by $(1-2e)$, one readily obtains the result

$$(1-f) = \frac{K^{\frac{1}{2}}\eta_\delta}{18\lambda^2 M^2}(1-\eta/\eta_\delta)^3. \tag{A 14}$$

This approximate solution enables the cubic variation of velocity with distance in the outer region to be readily discerned. A second set of inner solutions were computed by matching the numerical inner solution to (A 14) rather than to (A 12). The results were extremely close to the exact solutions; Reynolds numbers and friction factors differed by less than 0·3 % from the exact values over the range of acceleration parameters examined in this paper. This measure of agreement could have been anticipated because the velocity at the join was approximately $0{\cdot}9U$. The maximum error in the outer region resulting from linearizing the convective term was thus only about 1 %.

REFERENCES

Badri Narayanan, M. A. & Ramjee, V. 1968 On the criteria of reverse transition in a two-dimensional boundary layer flow. *India Inst. of Sci. Rep.* AE 68 FM 1.

Coles, D. 1962 Turbulent boundary layer in a compressible fluid. *RAND. Rep.* 403-PR.

Escudier, M. P. 1964 The distribution of mixing length in turbulent flows near walls. *Imperial College, Mech. Eng. Dept. Rep.* TWF/TN/1.

Hamel, G. 1917 Spiralformige Bewegungen zäher Flüssigkeiten. *Jber. dtsch. MatVer.* **25**, 34.

Herring, H. J. & Norbury, N. F. 1967 Some experiments on equilibrium turbulent boundary layers in favourable pressure gradient. *J. Fluid Mech.* **27**, 541.

Jeffrey, G. B. 1915 The two-dimensional steady motion of a viscous fluid. *Phil. Mag.* (6), **29**, 455.

Jones, W. P. 1967 Strongly accelerated turbulent boundary layers. M.Sc. Thesis, Imperial College.

Launder, B. E. 1964*a* Laminarisation of the turbulent boundary layer in a severe acceleration. *J. App. Mech.* **31**, 707.

Launder, B. E. 1964*b* Laminarisation of the turbulent boundary layer by acceleration. *M.I.T. Gas Turbines Lab. Rep.* no. 77.

Launder, B. E. & Stinchcombe, H. S. 1967 Non-normal similar boundary layers. *Imperial College, Mech. Eng. Dept. Rep.* TWF/TN/21.

Mellor, G. I. & Gibson, D. M. 1963 Equilibrium turbulent boundary layers. *Princeton University, Mech. Eng. Dept. Rep.* FLD 14.

Millsaps, K. & Pohlhausen, K. 1953 Thermal distribution in Jeffrey–Hamel flows between non-parallel plane walls. *J. Aero. Sci.* **20**, 187.

Moretti, P. M. & Kays, W. M. 1965 Heat transfer through an incompressible turbulent boundary layer with varying free-stream velocity and varying surface temperature. *Stanford University, Thermo. Sci. Div. Rep.* PG-1.

Patel, V. C. 1965 Calibration of the Preston tube and limitations on its use in pressure gradients. *J. Fluid Mech.* **23**, 185.

Patel, V. C. & Head, M. R. 1968 Reversion of turbulent to laminar flow. *Aero. Res. Counc.* 29 859—F.M. 3929.

Patankar, S. V. 1967 Heat and mass transfer in turbulent boundary layers. Ph.D. Thesis, University of London.

PATANKAR, S. V. & SPALDING, D. B. 1967 *Heat and Mass Transfer in Boundary Layers.* Morgan-Grampian.

POHLHAUSEN, K. 1921 Zur näherungsweisen Integration der Differentialgleichung der laminaren Grenzschicht. *Z. angew. Math. Mech.* **1**, 252.

ROSENHEAD, L. 1940 The steady two-dimensional radial flow of viscous fluid between two inclined plane walls. *Proc. Roy. Soc.* A **175**, 436.

SCHRAUB, F. A. & KLINE, S. J. 1965 A study of the structure of the turbulent boundary layer with and without longitudinal pressure gradients. *Stanford University, Thermo. Sci. Div. Rep.* MD–12.

TOWNSEND, A. A. 1956 *The Structure of Turbulent Shear Flow.* Cambridge University Press.

VAN DRIEST, E. R. 1956 On turbulent flow near a wall. *J. Aero. Sci.* **23**, 1007.